Highly stretchable and thermally healable polyampholyte hydrogels via hydrophobic modification

Gaukhar Toleutay, Esra Su, Sarkyt Kudaibergenov & Oguz Okay

Colloid and Polymer Science
Kolloid-Zeitschrift und Zeitschrift für Polymere

ISSN 0303-402X
Volume 298
Number 3

Colloid Polym Sci (2020) 298:273-284
DOI 10.1007/s00396-020-04605-8

Springer

Colloid and Polymer Science (2020) 298:273–284
https://doi.org/10.1007/s00396-020-04605-8

ORIGINAL CONTRIBUTION

Highly stretchable and thermally healable polyampholyte hydrogels via hydrophobic modification

Gaukhar Toleutay[1,2] · Esra Su[3] · Sarkyt Kudaibergenov[1,2] · Oguz Okay[3]

Received: 14 November 2019 / Revised: 23 December 2019 / Accepted: 19 January 2020 / Published online: 25 January 2020

Abstract

Aqueous solutions or gels of polyampholytes attract interest for more than half a century due to their several attractive properties. We present here thermally healable hydrophobically modified physical polyampholyte (PA) hydrogels based on oppositely charged 2-acrylamido-2-methylpropane-1-sulfonic acid sodium salt (AMPS) and (3-acrylamidopropyl) trimethylammonium chloride (APTAC) monomers. PA hydrogels were prepared via micellar polymerization technique in the presence of the hydrophobic monomer n-octadecyl acrylate (C18A) in aqueous sodium dodecyl sulfate (SDS) solutions. Charge-balanced PA hydrogels containing 60–90% water exhibit a high tensile strength and stretchability of up to 202 kPa and 1239%, respectively. Above 7 mol% C18A, swollen hydrogels containing around 90% water exhibit much better mechanical properties as compared with the corresponding as-prepared ones because of the stronger hydrophobic interactions in the absence of SDS micelles. Cut-and-heal tests conducted at 50 °C reveal a complete healing efficiency with respect to Young's modulus for all as-prepared PA hydrogels within 1–4 h.

Keywords Hydrogels · Polyampholytes · Hydrophobic interactions · Mechanical properties · Temperature-induced healing

Introduction

Polyampholytes, polymers carrying opposite charges, attract interest for more than half a century due to their several interesting properties such as their similarity to proteins and antipolyelectrolyte and isoelectric effects in aqueous solutions [1–9]. Among them, hydrophobically modified polyampholytes containing hydrophobic moieties at the side chain or in the polymer backbone are able to self-assemble into micelles, vesicles, lamellar aggregates, and so on [10, 11]. They have found several application areas including enhanced oil recovery, immobilization of metal catalysts, wax inhibitor, pour point depressant, drug/gene/protein delivery, and cryopreservation of living cells. Water-swollen cross-linked polyampholytes, i.e., polyampholyte (PA) hydrogels, also exhibit unique features such as their sensitivity against pH and salt concentration variations, low toxicity, good biocompatibility, and similarity to many biological systems and hence, they have a variety of applications including antibacterial, anti-fouling, and saline-resistant materials [12–22]. For instance, PA cryogels exhibit stimuli-responsive behavior and catalytic properties when metal nanoparticles are immobilized within the cryogel network [23].

PA hydrogels are mainly synthesized by free-radical copolymerization of cationic and anionic monomers in the presence of a chemical cross-linker [12–22]. However, such chemically cross-linked PA hydrogels exhibit poor mechanical performances such as a low modulus and tensile strength limiting their load-bearing applications. Hydrophobically modified

- Physical polyampholyte hydrogels are prepared via micellar polymerization technique.
- Incorporation of hydrophobes within the gel network provides their water stability.
- The hydrogels containing 60–90% water exhibit a high stretchability of up to 1239%.
- They exhibit a complete healing efficiency at 50 °C within 1–4 h.

Electronic supplementary material The online version of this article (https://doi.org/10.1007/s00396-020-04605-8) contains supplementary material, which is available to authorized users.

✉ Oguz Okay
okayo@itu.edu.tr

[1] Institute of Polymer Materials and Technology, Microregion "Atyrau 1", Bld. 3/1, Almaty, Kazakhstan 050019

[2] Satbayev University, Satpayev Str. 22, Almaty, Kazakhstan 050013

[3] Department of Chemistry, Istanbul Technical University, Maslak, 34469 Istanbul, Turkey

physical PA hydrogels with shape-memory function were recently synthesized by terpolymerization of acrylamide, acrylic acid, and a cationic surfmer (polymerizable surfactant) [24]. Gong et al. synthesized high-strength charge-balanced physical PA hydrogels with self-healing function via random copolymerization of cationic and anionic monomers at a high concentration [25, 26]. Formation of ionic bonds of various strengths due to the random distribution of charges along the polymer chains provided the formation of both permanent (strong) and sacrificial (weak) ionic bonds creating an effective energy dissipation that prevents crack propagation [25]. Physical PA hydrogels via hydrophobic and hydrogen bonding interactions were recently prepared by our group via terpolymerization of *N*,*N*-dimethylacrylamide, acrylic acid, and 4-vinylpyridine under solvent-free condition [27]. The hydrogels containing 80–92% water exhibit Young's moduli between 18 and 58 kPa and sustain tensile strains up to 560%.

Micellar polymerization technique first reported by Candau and co-workers is a versatile method for the copolymerization of hydrophilic and hydrophobic monomers leading to copolymers with a block-like structure [28–32]. By this technique, the micelle-solubilized hydrophobic monomer is copolymerized with a hydrophilic monomer in an aqueous solution by a free-radical mechanism. Due to the accumulation of the hydrophobic monomers within the surfactant micelles, they incorporate into the copolymer chains as blocks. This distinctive feature of micellar polymerization provides strengthening of hydrophobic interactions between the polymer chains as compared with those formed by random copolymerization. This technique is however limited to the hydrophobic monomers with alkyl side chains of less than 16 carbon atoms because larger hydrophobes cannot be solubilized within micelles [33]. Recently, it was shown that the solubilization of large hydrophobes such as n-octadecyl acrylate (C18A) can be achieved when, instead of monomeric micelles, worm-like micelles were used during the micellar polymerization [33]. For instance, although C18A is insoluble in aqueous 7 *w*/*v* % sodium dodecyl sulfate (SDS) solution, it can be solubilized if NaCl is included into the micellar solution which leads to micellar growth. This solubilization method provided strong hydrophobic interactions between hydrophobically modified hydrophilic chains leading to the formation of mechanically strong physical hydrogels with self-healing and shape-memory functions [33–37].

Here, we describe, for the first time to our knowledge, preparation of hydrophobically modified physical PA hydrogels via micellar polymerization in aqueous solutions of worm-like SDS micelles. 2-Acrylamido-2-methylpropane-1-sulfonic acid sodium salt (AMPS) and (3-acrylamidopropyl) trimethylammonium chloride (APTAC) were used as anionic and cationic monomers, respectively (Scheme 1). As will be seen below, micellar copolymerization of charge-balanced AMPS and APTAC in the presence of the hydrophobic monomer C18A without a chemical cross-linker leads to physical PA hydrogels with several unique features. The hydrogels containing 60–90% water sustain a high tensile strength (up to 202 kPa) and exhibit a high stretchability (up to 1239%). What is more, above 7 mol% C18A, swollen hydrogels containing around 90% water exhibit much better mechanical properties as compared with the corresponding as-prepared ones. Cut-and-heal tests conducted at 50 °C reveal a complete healing efficiency with respect to Young's modulus for all as-prepared PA hydrogels.

Experimental

Materials

The anionic and cationic monomers, 2-acrylamido-2-methylpropane-1-sulfonic acid sodium salt (AMPS, 50 wt%, Sigma-Aldrich) and (3-acrylamidopropyl) trimethylammonium chloride (APTAC, 75 wt%, Sigma-Aldrich), respectively, the hydrophobic monomer n-octadecyl acrylate (C18A, Sigma-Aldrich), sodium dodecyl sulfate (SDS, Sigma), sodium chloride (NaCl, Merck), chemical cross-linker *N*,*N*′-methylenebis (acrylamide) (BAAm, Merck), and initiator 2-oxoglutaric acid (Merck) were used as received.

Hydrogel preparation

Two sets of hydrogels were prepared by free-radical copolymerization of AMPS and APTAC under UV light in the presence of 2-oxoglutaric acid initiator (0.25 mol% with respect to the monomers). In the first set, the reactions were carried out via micellar copolymerization of equimolar AMPS and APTAC monomer mixture in the presence of the hydrophobic monomer C18A. Both the amount of C18A in the monomer mixture and the total monomer concentration C_o were varied between 1 and 25 mol% and between 1.0 and 2.5 M, respectively. An aqueous solution of SDS in 0.5 M NaCl was used as the micellar solution due to the significant solubilization power of the resulting worm-like SDS micelles [33, 35, 36]. SDS concentration was 7 and 14 *w*/*v* % for C18A contents below and above 10 mol%, respectively. Typically, to prepare hydrophobically modified hydrogels with 20 mol% C18A at $C_o = 1.0$ M, C18A (0.65 g) was first dissolved in 4.00 mL 0.5 M NaCl solution containing 1.40 g SDS at 35 °C for 2 h to obtain a homogeneous solution. The aqueous solutions of 50 wt% AMPS (2.29 g) and 75 wt% APTAC (1.38 g) were then added to the micellar solution of C18A and stirred for 30 min. After addition of 2-oxoglutaric acid (4 mg), the solution was transferred into plastic syringes of 4.6 mm in diameter to conduct the polymerization reactions at 23 ± 2 °C under UV light at $\lambda = 360$ nm for 24 h.

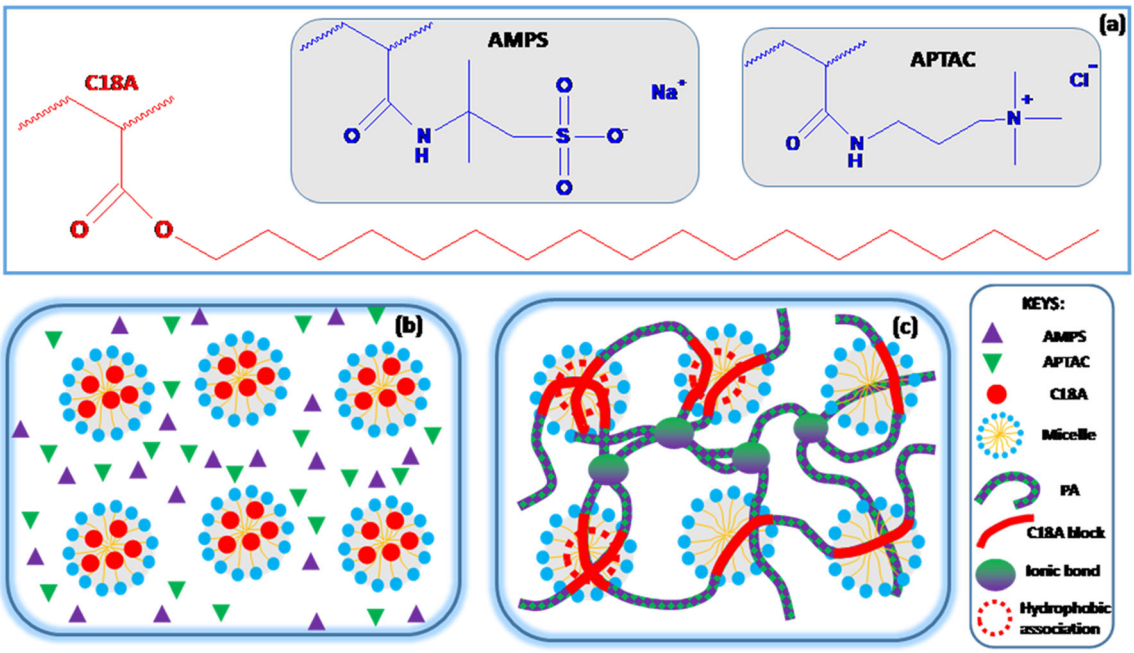

Scheme 1 (a) Structures of 2-acrylamido-2-methyl-1-propanesulfonic acid sodium salt (AMPS), (3-acrylamidopropyl) trimethyl ammonium chloride (APTAC), and n-octadecylacrylate (C18A) repeat units of physical polyampholyte hydrogels. (b, c) Scheme showing before (b) and after (c) gelation of the monomers via micellar polymerization method

In the second set of experiments, instead of C18A, the chemical cross-linker BAAm was used to prepare chemically cross-linked PA hydrogels. The amounts of BAAm and C_o were fixed at 1.25 mol%, with respect to the monomers, and 1.0 M, respectively, while AMPS mole fraction in the monomer mixture (x_{AMPS}) was varied. Typically, to prepare hydrogels at $C_o = 1.0$ M and $x_{AMPS} = 0.50$, the solutions of 50 wt% AMPS (2.29 g) and 75 wt% APTAC (1.38 g) were mixed in a glass vial and then, BAAm (20 mg) was dissolved in this solution at 35 °C under stirring. After adding distilled water to complete the solution volume to 10 mL followed by bubbling nitrogen gas for 10 min, 2-oxoglutaric acid (4 mg) initiator was added and the solution was transferred into plastic syringes of 4.6 mm in diameter to conduct the polymerization reactions under UV light as described above.

Hydrogel characterization

Hydrogels after preparation were cut into specimens of approximately 5 mm in length and placed in water at 23 ± 2 °C for at least 1 week during which water was refreshed every day. After attaining swelling equilibrium, they were freeze-dried and the gel fraction W_g, equilibrium weight swelling ratio $m_{rel,eq}$ with respect to the as-prepared state, and the water content (W) of swollen hydrogels were calculated as follows:

$$W_g = \frac{m_{dry}}{m_o w_M} \quad (1a)$$

$$m_{rel,eq} = \frac{m_s}{m_o} \quad (1b)$$

$$W\ \% = 10^2 \left(1 - \frac{w_M W_g}{m_{rel}}\right) \quad (1c)$$

where m_{dry}, m_o, and m_s are the masses of hydrogels in dry, as-prepared, and equilibrium swollen states, respectively, and w_M is the mass fraction of the monomers in the reaction solution without SDS and NaCl. Water content W of as-prepared hydrogels was calculated from the composition of the reaction solutions.

Rheological tests were carried out on a rheometer system (Gemini 150, Bohlin Instruments) equipped with a Peltier device for temperature control and a solvent trap to prevent water evaporation. Hydrogel specimens in their as-prepared states were cut into slices of about 3 mm in thickness and 20 mm in diameter. They were then introduced between the parallel plates of the rheometer and the spacing was set to 2950 ± 150 μm. The dynamic moduli of the hydrogels were recorded at 25 °C and at a strain amplitude γ_o of 1% over the frequency range 0.3 to 135 rad s^{-1}.

The mechanical tests were carried out at 23 ± 2 °C on a Zwick Roell Z0.5 TH test machine with a 500-N load cell. Cylindrical hydrogel specimens of 4.6 mm in diameter were subjected to uniaxial compression and elongation measurements at a strain rate of 1 min^{-1}, as detailed before [27]. The nominal σ_{nom} and true stresses σ_{true} (= $\lambda\ \sigma_{nom}$) were recorded, which represent the forces per cross-sectional area of the undeformed and deformed specimen, respectively, and λ is the deformation ratio (deformed length/initial length). For the

strain ε, the change in the length of the specimen with respect to its initial length was calculated as $\varepsilon = \lambda - 1$ and $\varepsilon = 1 - \lambda$, for elongation and compression, respectively. Young's modulus E was calculated from the slope of the nominal stress-strain curves between 5 and 15% deformation. The compressive strength σ_f was calculated from the maxima in true stress-strain curves, as detailed before [38]. Cyclic tensile experiments were conducted at a strain rate of 5 min^{-1} to a maximum strain ε_{max} of 200 or 600%, followed by immediate retraction to zero displacement and a waiting time of 1 min and 2 min, respectively, until the next cycle of tensile. The mechanical parameters and the water contents of as-prepared and swollen hydrogels are compiled in Table 1.

To quantify the healing efficiency of the hydrogels, cut-and-heal tests were carried out on gel specimens in cylindrical forms of 4.6 mm in diameter and 1 cm in length. The gel specimens were first cut in their middle and then, the two gel parts were merged within a plastic syringe (of the same diameter as the gel sample) by slightly pressing the piston plunger at 50 °C for various healing times between 1 and 24 h. The efficiency of healing was calculated from the ratios of Young's modulus and fracture stress of the healed samples to those of the virgin ones.

Results and discussion

Hydrophobically modified polyampholyte (PA) hydrogels were prepared using equimolar amounts of AMPS and APTAC monomers without a chemical cross-linker via micellar polymerization in the presence of the hydrophobic monomer C18A (Scheme 1). Before highlighting the extraordinary properties of hydrophobically modified PA hydrogels, we first present the behavior of the classical, chemically cross-linked PA hydrogels prepared at various mole fractions of AMPS in the comonomer feed. In the following subsections, we discuss the properties of the physical PA hydrogels prepared at various hydrophobic monomer contents.

Chemically cross-linked polyampholyte hydrogels

Chemically cross-linked PA hydrogels were prepared from oppositely charged AMPS and APTAC monomers at various mole fractions x_{AMPS} of AMPS between 0 and 1 in the comonomer feed. They were synthesized at a total monomer concentration C_M of 1.0 M in the presence of 1.25 mol% BAAm cross-linker. Figure 1 (a) shows the equilibrium weight swelling ratio $m_{rel,eq}$, and the gel fraction W_g of the hydrogels plotted against x_{AMPS}. W_g equals to 0.66 and 0.9 in the absence and presence of AMPS, respectively, whereas it becomes unity at $x_{AMPS} = 1$. The increase in the gel fraction after incorporation of AMPS segments into the gel network could be attributed to the formation of hydrogen bonds between the polymer chains contributing to the cross-link density of the hydrogels [39]. As expected, visual observation showed that the hydrogels assume their most compacted state at $x_{AMPS} = 0.5$ (Fig. 1(b)). At this state, the degree of swelling $m_{rel,eq}$ of the hydrogel is 14- and 11-fold smaller than that formed at $x_{AMPS} = 0$ and 1, respectively, due to the charge balance of the comonomer units.

All as-prepared hydrogels were too brittle in tension and hence, they cannot be subjected to uniaxial tensile tests. Therefore, uniaxial compression tests were performed at a constant strain rate of 1 min^{-1} (Fig. S1). Figure 1 (c) shows Young's modulus E and compressive fracture stress σ_f of the hydrogels as a function of x_{AMPS}. At $x_{AMPS} = 0.5$, the modulus E attains a maximum value (63 ± 3 kPa) while the fracture stress σ_f exhibits a minimum, i.e., below 2 MPa, due to the ionic bonds between AMPS and APTAC segments acting as cross-links in addition to the chemical BAAm ones, as well as low amount of water in the charge-balanced hydrogel. The results thus reveal poor mechanical properties of PA hydrogels

Table 1 Water content (W %), Young's modulus E, tensile strength σ_f, and elongation at break ε_f of as-prepared and water-swollen PA hydrogels at various C18A contents

C18A mol%	W %		E/kPa		σ_f/kPa		ε_f %	
	As-prepared	Swollen	As-prepared	Swollen	As-prepared	Swollen	As-prepared	Swollen
1	71 (3)	soluble	14 (3)	–	34 (1)	–	1403 (155)	–
2	71 (2)	88 (2)	22 (3)	2 (1)	40 (1)	8 (1)	1239 (162)	464 (49)
5	70 (3)	90 (1)	23 (1)	9 (2)	40 (1)	68 (14)	910 (47)	523 (27)
7	69 (3)	88 (1)	31 (2)	19 (2)	59 (10)	103 (9)	921 (3)	484 (36)
10	64 (2)	90 (1)	45 (6)	65 (7)	75 (5)	112 (13)	929 (146)	490 (50)
15	63 (2)	86 (1)	64 (7)	76 (2)	99 (10)	122 (20)	779 (45)	331 (34)
20	61 (1)	87 (1)	99 (8)	97 (11)	145 (15)	213 (27)	662 (16)	257 (14)
25	60 (1)	87 (1)	103 (7)	174 (25)	172 (9)	202 (24)	608 (11)	137 (22)

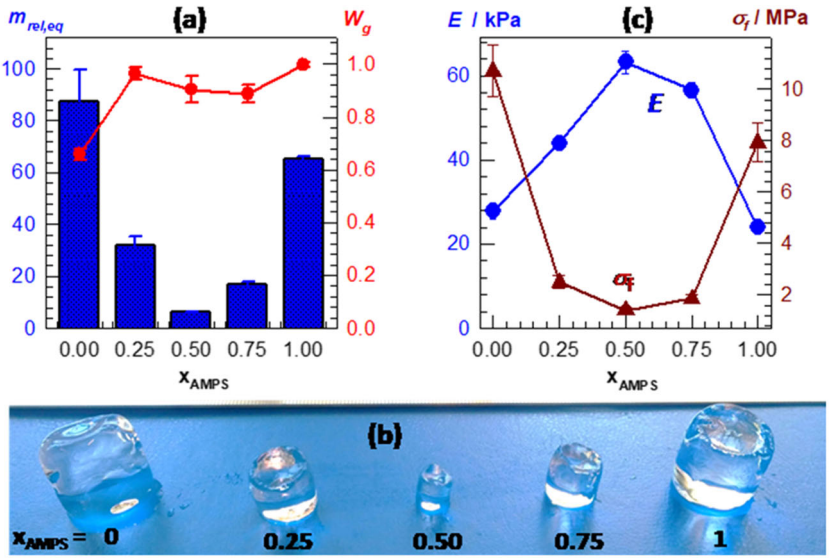

Fig. 1 (a) The equilibrium weight swelling ratio $m_{rel,eq}$, and the gel fraction W_g of the hydrogels plotted against x_{AMPS}. (b) Young's modulus E and compressive fracture stress σ_f of the hydrogels shown as a function of x_{AMPS}. (c) Images of water-swollen polyampholyte hydrogels with various AMPS contents

because of the absence of an effective energy dissipation mechanism in the chemically cross-linked PA network. In the following, we fix the comonomer composition at $x_{AMPS} = 0.5$, whereas no chemical cross-linker was used the gel preparation.

Hydrophobically modified physical polyampholyte hydrogels

Instead of the chemical cross-linker BAAm producing brittle PA hydrogels, the hydrophobic monomer n-octadecyl acrylate (C18A) was incorporated into the backbone of PA chains to create hydrophobic associations between alkyl side chains of C18A units. We observed that even the addition of a small amount of C18A leads to gel formation. For instance, the images in Fig. 2 (a) and (b) show charge-balanced physical hydrogels formed at various monomer concentrations C_M without and with 2 mol% C18A in the comonomer feed, respectively. With C18A, a physical gel could be obtained at the lowest monomer concentration C_M of 1.0 M, while, without C18A, no gel forms below $C_M = 2.5$ M. The appearance of opacity in hydrophobically modified polyampholyte hydrogels reveals existence of submicro-sized domains of hydrophobic associations. To investigate in detail, we fixed the monomer concentration C_M at 1.0 M and varied the amount of C18A in the comonomer mixture between 5 and 20 mol%.

Figure 3 shows angular frequency (ω) dependences of the storage modulus (G'), loss modulus (G''), and loss factor (tan δ) of charge-balanced hydrogels in their as-prepared states, formed at $C_M = 1.0$ M and at various C18A contents. The dynamic moduli and tan δ of the hydrogel without C18A are shown by the open symbols and dashed line, respectively. Incorporation of C18A into the hydrogel leads to an increase of G' from Pa to kPa level and its frequency dependence decreases. For instance, G' at 10 rad s^{-1} is 0.4 kPa in the absence of C18A, while around two orders of magnitude increases at 25 mol% C18A (31 kPa). Moreover, tan δ remains above 0.1 for all hydrophobically modified PA hydrogels revealing the existence of dynamic cross-links and hence their viscous character. The physical gels formed above 1 mol% C18A were insoluble in water, similar to their chemically cross-linked analogs as discussed in the previous section. Figure 4 (a) shows the equilibrium swelling ratio $m_{rel,eq}$, and the gel fraction W_g of the hydrogels plotted against their hydrophobe contents. W_g is above 0.8 and it increases with increasing C18A content from 2 to 25 mol%. Moreover, the swelling ratio of hydrophobically modified PA hydrogels is 2.5 ± 0.4 and almost independent on the amount of C18A, as

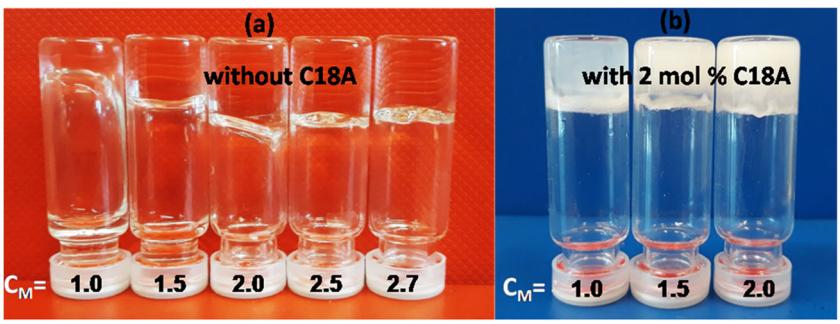

Fig. 2 Images of charge-balanced PA hydrogels at various monomer concentrations C_M without (a) and with (b) 2 mol% C18A

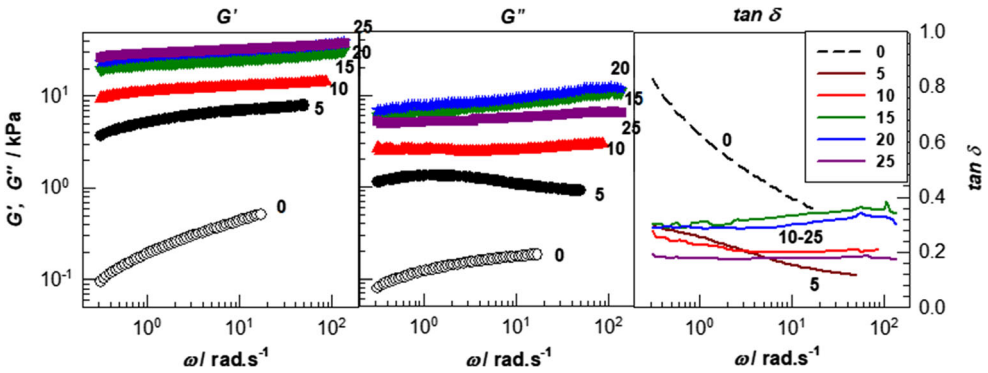

Fig. 3 Storage modulus G', loss modulus G'', and loss factor tan δ of charge-balanced hydrogels shown as a function of the angular frequency ω. $C_M = 1.0$ M. C18A contents are indicated

compared with 6.1 ± 0.2 for chemically cross-linked PA hydrogel at the same AMPS mole fraction (Fig. 1(a)). The lower swelling ratio after hydrophobic modification is attributed to the increased hydrophobicity of the resulting hydrogels.

Another characteristic feature of hydrophobically modified PA hydrogels was their unusual swelling kinetics in water, as shown in Fig. 4(b). The swelling ratio m_{rel} of the hydrogels first increases up to a maximum value ($m_{rel,max}$) within 1 day, while at longer swelling times, they start to deswell until attaining their swelling equilibrium after 10 days. Moreover, the lower the C18A content, the higher is $m_{rel,max}$ of the hydrogel. Similar swelling kinetics was reported before for non-ionic polyacrylamide hydrogels prepared via micellar polymerization in aqueous SDS solutions [33]. The present hydrophobically modified PA hydrogels are charge-balanced and hence, their polymer networks are also non-ionic. However, they behave as ionic ones when immersed in water due to the existence of Na^+ counterions of the surfactant SDS inside the gel network. Because of the osmotic pressure of SDS counterions, they significantly swell in water, as seen during the 1st day of the swelling time (Fig. 4(b)). However, as SDS is extracted from the hydrogels, they gradually turn into non-ionic ones so that their swelling ratio decreases at longer times. As will be seen below, the cross-link density (ν_e) of the hydrogels decreases with decreasing amount of C18A (Fig. 6(b)). Thus, at a low cross-link density, the diffusion of water inside the gel network is faster than the extraction of SDS from the hydrogel so that the hydrogels with low C18A contents exhibit high maximum swelling ratios $m_{rel,max}$.

In contrast to the chemically cross-linked PAs presented in the previous section, all hydrophobically modified PAs were highly stretchable and the stretch ratio at break varied depending on the C18A content, and on the gel state during the tensile tests. Figure 5 (a) and (b) show tensile stress-strain curves of as-prepared and water-swollen hydrogels, respectively. The results of the water-soluble hydrogels with < 2 mol% C18A are shown by the dashed curves in Fig. 5(a). Young's modulus E, tensile strength σ_f, and elongation ratio at break ε_f of the hydrogels are compiled in Fig. 5(c) and Table 1 as a function of C18A mol%. The modulus E and tensile strength σ_f increase with increasing hydrophobe content for both as-prepared and swollen hydrogels and they become 175 ± 25 and 202 ± 24 kPa, respectively, for swollen hydrogels with 25 mol% C18A. The open circle in Fig. 5(c) representing the modulus E of the chemically cross-linked charge-balanced PA hydrogel in the as-prepared state reveals that, above 10 mol% C18A, hydrophobically modified physical PA hydrogels are much stiffer than the chemical hydrogel in both as-prepared and swollen states. The stretch at break (ε_f) is a decreasing function of C18A content and varies between 137 and 1400%.

An interesting point from Fig. 5(c) and Table 1 is that the swollen hydrogels at high C18A contents are stiffer than in

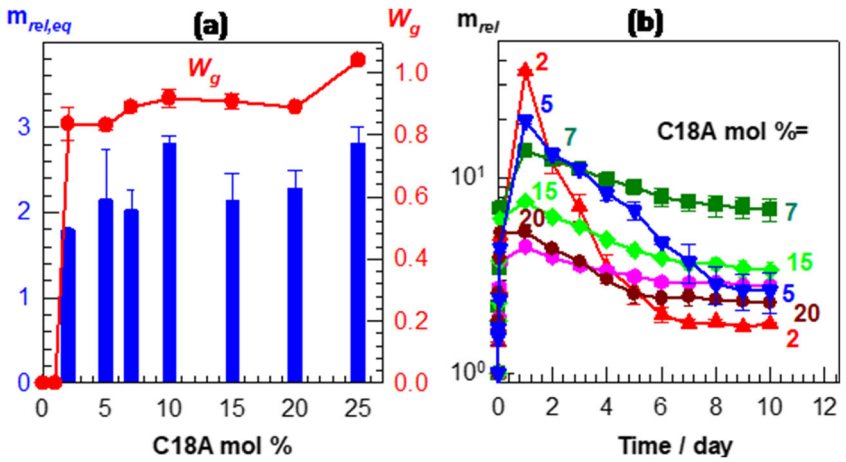

Fig. 4 (a) The equilibrium weight swelling ratio $m_{rel,eq}$, and the gel fraction W_g of the physical hydrogels plotted against C18A mol %. (b) The weight swelling ratio m_{rel} plotted against the time of swelling of the hydrogels with various C18A contents

their as-prepared states. This finding is unexpected as swelling of the hydrogels increases their water contents and hence decreases the number of elastically effective cross-links in a unit gel volume. For instance, at 25 mol% C18A, although the water content of the hydrogel increases from 60 to 87 ± 1% upon swelling in water (Fig. 6(a)), its modulus E also increases from 103 to 175 kPa. This behavior is attributed to the presence of surfactant in as-prepared hydrogels. Surfactant micelles are known to weaken hydrophobic interactions due to their solubilization effect and hence, they decrease the lifetime of hydrophobic associations [33]. This results in a decrease in the effective cross-link density of the hydrogels formed via micellar polymerization [34]. To verify this hypothesis, the effective cross-link density ν_e of the hydrogels, i.e., the number of network chains per volume of dry cross-linked polymer, was calculated using the theory of elasticity as [40, 41]

$$E = 3\,\nu_e\,R\,T\,(\nu_2)^{1/3}\,\left(\nu_2^0\right)^{2/3} \quad (2)$$

where ν_2^0 and ν_2 are the volume fractions of cross-linked polymer at the state of gel preparation and during the mechanical tests, respectively, R is the gas constant and T is the absolute temperature. Using the water contents (W) shown in Fig. 6(a), ν_2^0 and ν_2 of the hydrogels were calculated as d_p^{-1} $(1 - W)$ where d_p is the polymer density which was taken as the density of PAMPS (1.44 g mL^{-1} [42]). Figure 6 (b) shows the calculated cross-link densities ν_e of PA hydrogels in their as-prepared and swollen states plotted against C18A mol%. ν_e of swollen hydrogels containing ≥ 10 mol% C18A is higher than that in their as-prepared states reflecting the strengthening of hydrophobic interactions in the absence of surfactants.

In addition to the C18A amount, the mechanical properties of hydrophobically modified PA hydrogels can also be tuned by varying the monomer concentration C_M at the gel preparation at a fixed C18 mol%. For instance, with increasing C_M from 1.0 to 2.0 M at 2 mol% C18A, both E and σ_f increased from 2 to 16 ± 2 kPa and 8 to 89 ± 13 kPa, respectively, whereas the stretch at break was slightly reduced from 1100 to 900% (Fig. S2). The 8-fold increase in the modulus by doubling the concentration C_M reveals the increasing extent of hydrophobic interactions between hydrophobically modified PA chains at high concentrations.

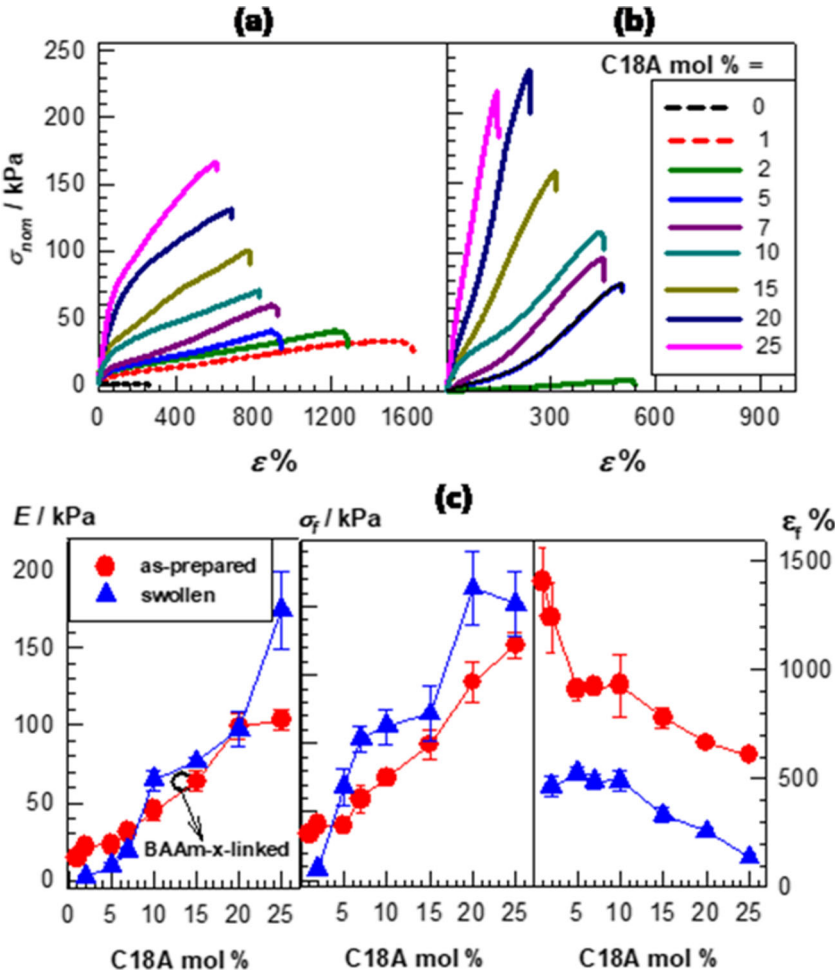

Fig. 5 (a, b) Tensile stress-strain curves of hydrophobically modified physical PA hydrogels in as-prepared (a) and water-swollen (b) states at various C18A contents. (c) The modulus E, tensile strength σ_f, and elongation ratio at break ε_f of the hydrogels plotted against C18A mol%. The open circle in the left panel represents the modulus of chemically cross-linked charge-balanced PA hydrogel

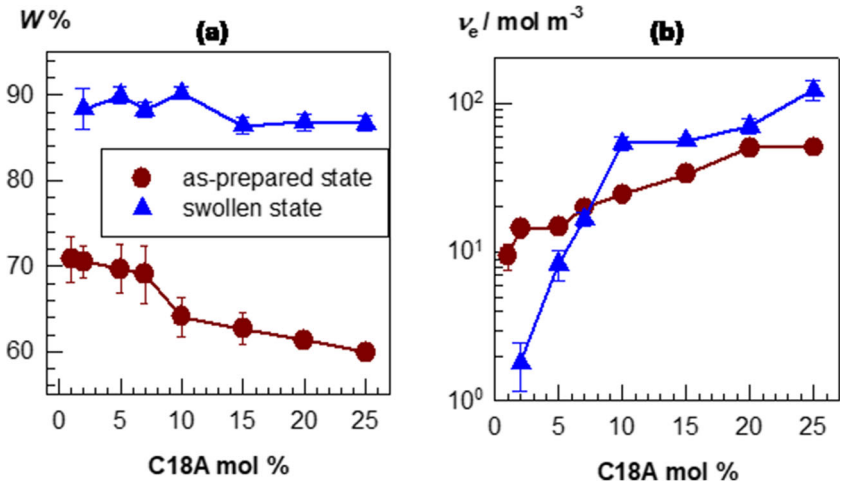

Fig. 6 (a, b) The water contents W (a) and cross-link density ν_e (b) of hydrophobically modified physical PA hydrogels in as-prepared (circles) and swollen states (triangles) plotted against C18A mol%

Temperature-induced healing behavior

Because hydrophobically modified PA hydrogels have poly (AMPS-co-APTAC) chains interconnected by non-covalent bonds, one may expect that they all have the ability to self-heal after damage. Cut-and-heal tests indeed revealed the healing behavior of all as-prepared hydrogels at an elevated temperature, whereas those prepared via chemical cross-linker BAAm described in the first subsection cannot be healed. Cyclic mechanical tests are a mean to understand the nature and reversibility of the intermolecular bonds in the hydrogels. Figure 7 (a) and (b) show typical cyclic tensile stress-strain

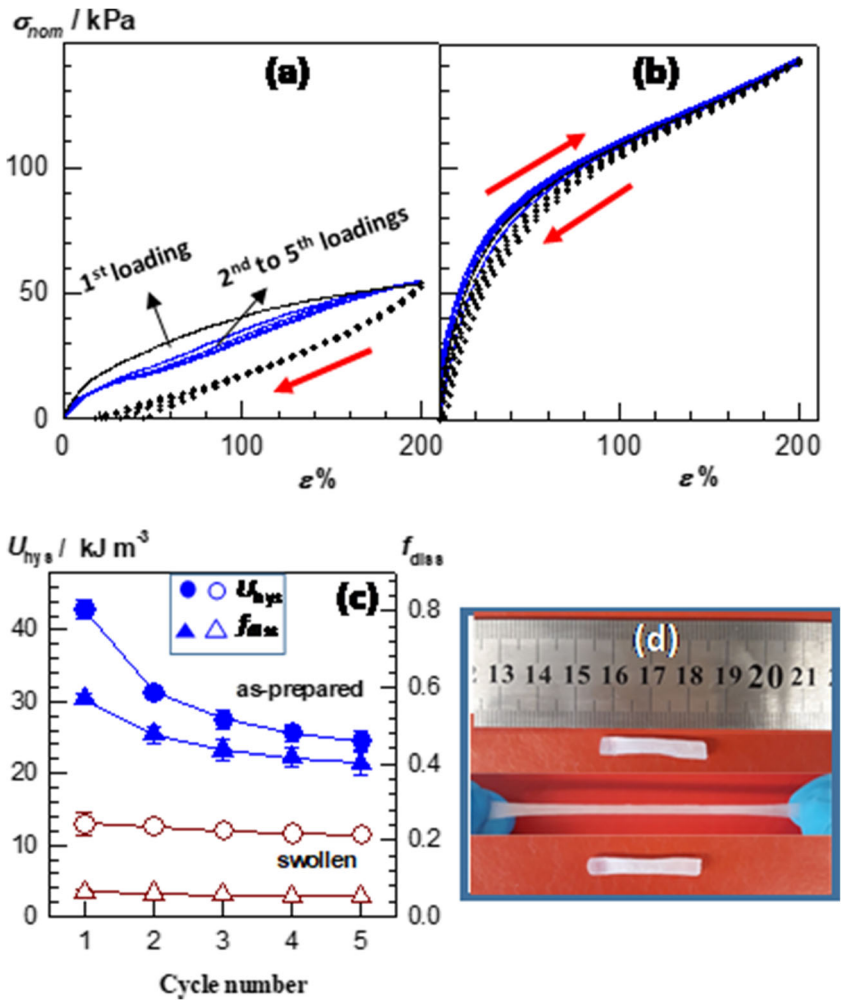

Fig. 7 (a, b) Five successive cyclic tensile test results conducted on a gel specimen with 20 mol% C18A in its as-prepared (a) and swollen (b) states. Loading and unloading steps are shown by solid and dotted curves, respectively. Waiting time between cycles = 1 min. (c) Hysteresis energies U_{hys} (circles) and fraction f_{diss} of dissipated energy (triangles) plotted against C18A mol%. (d) Images of a hydrogel specimen with 5 mol% C18A demonstrating its self-recoverability after stretching to 500% elongation

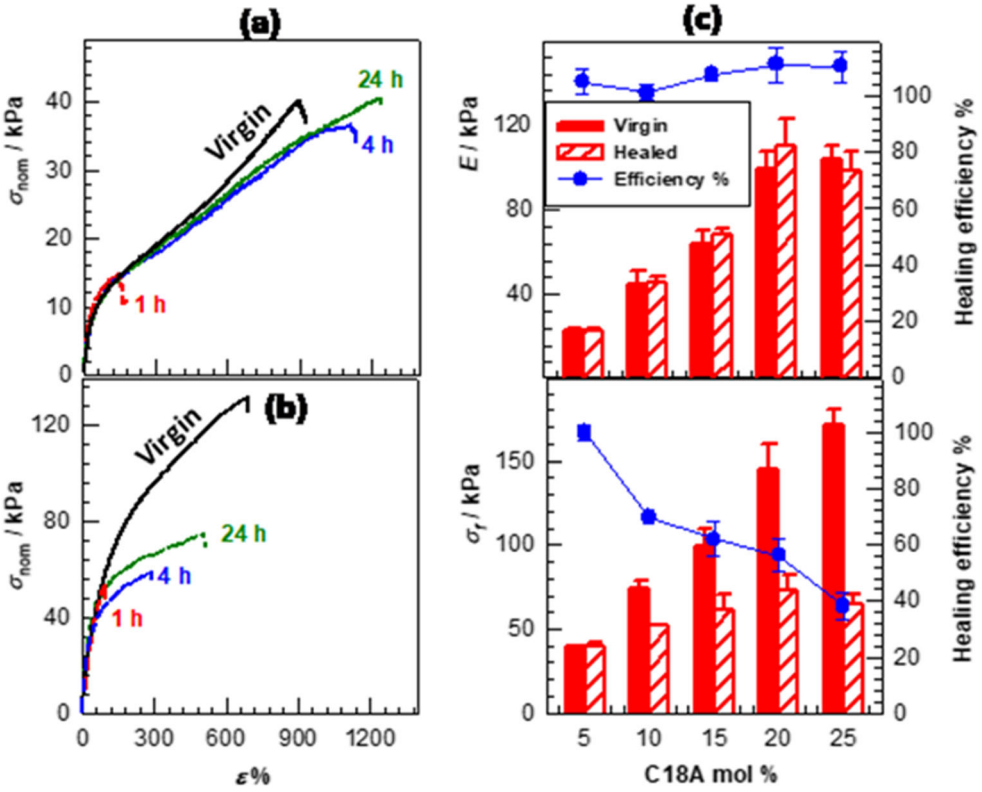

Fig. 8 (a, b) Stress-strain curves of virgin and healed PA hydrogels. C18A = 5 (a) and 20 mol% C18A (b). Healing times at 50 ± 2 °C are indicated. (c) E (upper panel) and σ_f (bottom panel) of virgin and healed hydrogels, and the healing efficiencies (blue circles) shown as a function of C18A mol%. Healing time = 24 h

curves of a gel specimen with 20 mol% C18A in its as-prepared and swollen states, respectively. During the tensile tests, the specimens were first stretched to 200% elongation at a fixed strain rate of 5 min^{-1} and then unloaded at the same rate to zero stress. These loading and unloading steps shown in the figures by solid and dotted curves, respectively, were repeated 4 times with a waiting time of 1 min between the cycles.

A negative deviation of all unloading curves from the loadings is seen in the figures reflecting the occurrence of damage in the intermolecular bonds during stretching. The hysteresis energy U_{hys}, i.e., the area surrounded by the loading and

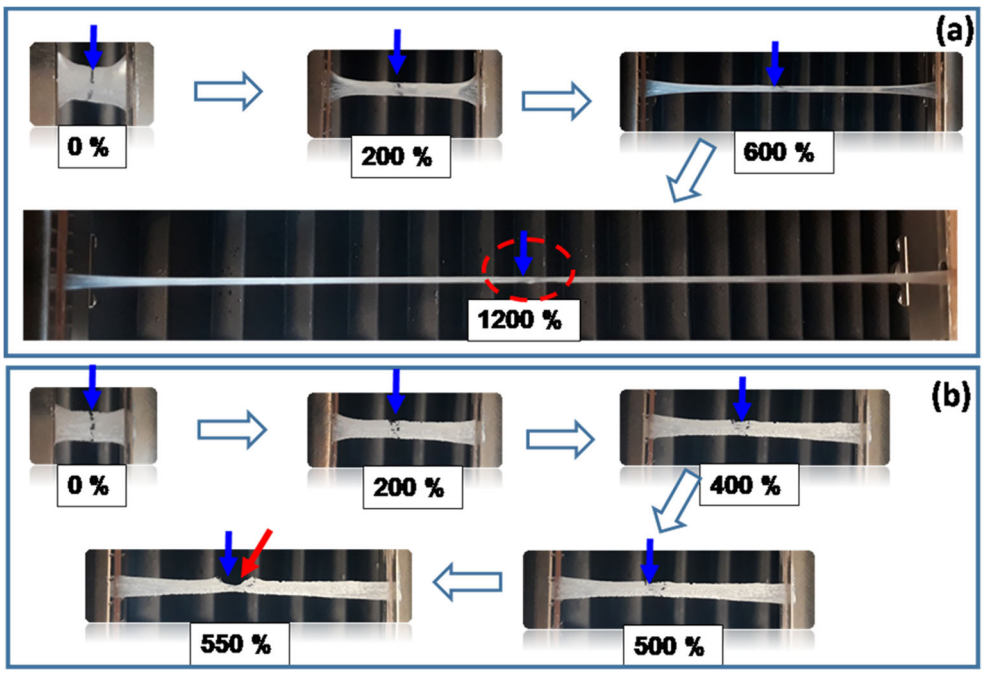

Fig. 9 Images of healed hydrogel specimens with 5 (a) and 20 mol% (b) C18A during stretching. Healing time at 50 ± 2 °C = 24 h. Healed areas, indicated by blue arrows, were colored with a dye for clarity. The locations of the fracture points are indicated by red dashed circle, and red arrow for (a) and (b), respectively

unloading curves, is much larger in the as-prepared state as compared with that in the swollen state, and it decreases with the cycle number, as seen in Fig. 7(c). This reveals that a much larger number of bonds are broken in as-prepared hydrogels which is attributed to their weakness because of the surfactant micelles. Similar to the surfactant micelles, ethanol is a good solvent for C18A segments able to solubilize their associations. We also conducted successive cyclic tensile tests on the hydrogel with 20 mol% C18A equilibrium swollen in ethanol (Fig. S3). We found that U_{hys} significantly increases when measured from ethanol-swollen hydrogels as compared with both as-prepared and water-swollen hydrogels, thus supporting our finding. The fraction of energy dissipated per loading energy f_{diss} is 40–57% and 6% for the as-prepared and swollen hydrogels, respectively, revealing that the hydrogels containing surfactant have a much more effective energy dissipation mechanism as compared without surfactant (Fig. 7(c)). This also predicts that only PA hydrogels in their as-prepared states will have the ability to heal after damage. Another feature of the hydrogels is their excellent self-recoverability in a short period of time after deformation. For instance, Fig. 7 (d) shows images of a gel specimen with 5 mol% C18A during stretching to 500% deformation and just after unloading. The specimen recovers its initial length within seconds. This also highlights good elastic behavior of the hydrogels due to the existence of dual intermolecular interactions, namely ionic interactions between AMPS and APTAC segments and hydrophobic interactions between the polymer chains via C18A associations.

To highlight the healing behavior of PA hydrogels, cut-and-heal tests were conducted at 50 ± 2 °C and at various healing times between 1 and 24 h. As expected from the cyclic tensile test results, no healing could be detected in water-swollen hydrogels due to the existence of strong ionic and hydrophobic interactions. However, they could easily be healed in their as-prepared states. Figure 8 (a) and (b) show stress-strain curves of virgin and healed as-prepared hydrogels containing 5 and 20 mol% C18A, respectively, after various healing times. The recovery of the original modulus after cut-and-heal tests was complete within 1–4 h for both hydrogels. However, the healing with respect to ultimate properties required longer healing times. For instance, after 1 day of healing, the healing efficiency with respect to the tensile strength is 100 and 56 ± 6% for hydrogels with 5 and 20 mol% C18A, respectively. In Fig. 8(b), the modulus E and tensile strength σ_f of virgin and 1-day healed hydrogels together with the healing efficiencies are shown as a function of C18A mol%. Independent on the hydrophobe content, the healing efficiency with respect to the modulus E, i.e., the stiffness of the hydrogels, is complete, revealing recovery of the virgin network structure and the cross-link density. However, recovery of tensile strength σ_f continuously decreases with increasing C18A content and reduces to 40% at 25 mol% C18A.

Different healing behaviors of the initial and ultimate mechanical properties of as-prepared PA hydrogels suggest that, although the virgin microstructure is recovered after healing, some weak points remain in the gel specimens leading to crack propagation at lower strains. It was found that these weak points locate at or in the vicinity of the cut regions of the healed hydrogels. For instance, Fig. 9 (a) and (b) show images of 1-day healed hydrogels with 5 and 20 mol% C18A, respectively, during stretching up to their fracture points. The healed cut regions are indicated by the blue arrows. 5 mol% C18A hydrogel sustaining up to around 1200% strain and exhibiting a complete healing efficiency fractured at any location in the middle of the gel specimens, as indicated by red circle. In contrast, the fracture of 20 mol% C18A hydrogel occurred at the healed region, as indicated by a red arrow, revealing the existence of microcracks at the cut surfaces.

Conclusions

PA hydrogels exhibit unique features such as sensitivity against pH and salt concentration variations, low toxicity, good biocompatibility, and similarity to many biological systems and hence, they have a variety of applications including antibacterial, anti-fouling, and saline-resistant materials. However, PA hydrogels generally exhibit poor mechanical properties such as a low modulus and tensile strength limiting their load-bearing applications. We presented here thermally healable hydrophobically modified physical PA hydrogels based on oppositely charged AMPS and APTAC monomers. PA hydrogels were prepared via micellar polymerization technique in the presence of n-octadecyl acrylate (C18A) as the hydrophobic monomer in aqueous solutions of SDS micelles. Charge-balanced PA hydrogels containing 60–90% water sustain a high tensile strength (up to 202 kPa) and exhibit a high stretchability (up to 1239%). Above 7 mol% C18A, swollen hydrogels containing around 90% water exhibit much better mechanical properties as compared with the corresponding as-prepared ones because of the stronger hydrophobic interactions in the absence of surfactant micelles. Cut-and-heal tests conducted at 50 °C reveal complete recovery of Young's modulus of all as-prepared hydrogels within 1–4 h. However, healing of ultimate properties such as tensile strength was incomplete and required longer healing times due to some weak points remaining in the healed hydrogels. The present results thus show that the incorporation of hydrophobic C18A blocks into PA backbone via micellar polymerization increases the mechanical performance of the resulting PA hydrogels and creates temperature-induced healing behavior. One may think that a blockwise distribution of charges along the PA backbone would further enhance the mechanical performance of hydrophobically modified PA hydrogels. This could be achieved if one of the oppositely charged monomers

has hydrophobic groups so that it could be dissolved in surfactant micelles together with C18A.

Acknowledgments E.S. thanks Science Fellowships and Grant Programmes (BIDEB) of the Scientific and Technological Research Council of Turkey (TUBITAK) for a Ph.D. scholarship. O. O. thanks Turkish Academy of Sciences (TUBA) for the partial support.

Funding information The work was supported by Ministry of Education and Science of the Republic of Kazakhstan (IRN AP05131003, 2018–2020).

Compliance with ethical standards

Conflict of interest The authors declare that they have no conflict of interest.

References

1. Alfrey JT, Morawetz H, Fitzgerald EB, Fuoss RM (1950) Synthetic electrical analog of proteins. J Am Chem Soc 72:1864–1864
2. Katchalsky A, Miller IR (1954) Polyampholytes. J Polym Sci 13: 57–68
3. Patrickios CS, Hertler WR, Abbott NL, Hatton TA (1994) Diblock, ABC triblock, and random methacrylic polyampholytes: synthesis by group transfer polymerization and solution behavior. Macromolecules 27:930–937
4. Kudaibergenov SE (2002) Polyampholytes: synthesis, characterization and application. Plenum, New York
5. Lowe AB, McCormick CL (2002) Synthesis and solution properties of zwitterionic polymers. Chem Rev 102:4177–4189
6. Lowe AB, McCormick CL (2006) Eds., Polyelectrolytes and polyzwitterions: synthesis, properties and applications; ACS Symposium Series, American Chemical Society: Washington, 937
7. Kudaibergenov SE, Nuraje N, Khutoryanskiy VV (2012) Amphoteric nano-, micro-, and macrogels, membranes and thin films. Soft Matter 8:930–9321
8. Zurick KM, Bernards M (2014) Recent biomedical advances with polyampholyte polymers. J Appl Polym Sci 131. https://doi.org/10.1002/app.40069
9. Kudaibergenov SE, Ciferri A (2007) Natural and synthetic polyampholytes 2. Functions and applications. Macromol Rapid Commun 28:1969–1986
10. Kudaibergenov S, Koetz J, Nuraje N (2018) Nanostructured hydrophobic polyampholytes: self-assembly, stimuli-sensitivity, and application. Adv Comp Hybrid Mater 1:649–684
11. Rullens F, Devillers M, Laschewsky A (2004) New regular, amphiphilic poly (ampholyte)s: synthesis and characterization. Macromol Chem Phys 205:1155–1166
12. Baker JP, Stephens DR, Blanch HW, Prausnitz JM (1992) Swelling equilibria for acrylamide-based polyampholyte hydrogels. Macromolecules 25:1955–1958
13. Baker JP, Blanch HW, Prausnitz JM (1995) Swelling properties of acrylamide-based ampholytic hydrogels: comparison of experiment with theory. Polymer 36:1061–1069
14. Annaka M, Tanaka T (1992) Multiple phases of polymer gels. Nature 355:430–432
15. Mafe S, Manzanares JA, English AE, Tanaka T (1997) Multiple phases in ionic copolymer gels. Phys Rev Lett 79:3086–3089
16. Dogu S, Kilic M, Okay O (2009) Collapse of acrylamide-based polyampholyte hydrogels in water. J Appl Polym Sci 113:1375–1382
17. Gao M, Gawel K, Stokke BT (2014) Polyelectrolyte and antipolyelectrolyte effects in swelling of polyampholyte and polyzwitterionic charge balanced and charge offset hydrogels. Eur Polym J 53:65–74
18. Carr LR, Xue H, Jiang S (2011) Functionalizable and nonfouling zwitterionic carboxybetaine hydrogels with a carboxybetaine dimethacrylate crosslinker. Biomaterials 32:961–968
19. Liu SQ, Yang C, Huang Y, Ding X, Li Y, Fan WM, Hedrick JL, Yang YY (2012) Antimicrobial and antifouling hydrogels formed in situ from polycarbonate and poly (ethylene glycol) via Michael addition. Adv Mater 24:6484–6489
20. Mi L, Jiang S (2012) Synchronizing nonfouling and antimicrobial properties in a zwitterionic hydrogel. Biomaterials 33:8928–8933
21. Constantinou AP, Elladiou M, Patrickios CS (2016) Regular and inverse polyampholyte hydrogels: a detailed comparison. Macromolecules 49:3869–3880
22. Grinberg VY, Burova TV, Grinberg NV, Alvarez-Lorenzo C, Khokhlov AR (2019) Protein-like energetics of conformational transitions in a polyampholyte hydrogel. Polymer 179:121617
23. Kudaibergenov S (2019) Physicochemical, complexation and catalytic properties of polyampholyte cryogels. Gels 5:8
24. Fan Y, Zhou W, Yasin A, Li H, Yang H (2015) Dual-responsive shape memory hydrogels with novel thermoplasticity based on a hydrophobically modified polyampholyte. Soft Matter 11:4218–4225
25. Sun TL, Kurokawa T, Kuroda S, Ihsan AB, Akasaki T, Sato K, Haque A, Nakajima T, Gong JP (2013) Physical hydrogels composed of polyampholytes demonstrate high toughness and viscoelasticity. Nat Mater 12:932–937
26. Ihsan AB, Sun TL, Kurokawa T, Karobi SN, Nakajima T, Nonoyama T, Roy CK, Luo F, Gong JP (2016) Self-healing behaviors of tough polyampholyte hydrogels. Macromolecules 49:4245–4252
27. Su E, Okay O (2017) Polyampholyte hydrogels formed via electrostatic and hydrophobic interactions. Eur Polym J 88:191–204
28. Candau F, Selb J (1999) Hydrophobically-modified polyacrylamides prepared by micellar polymerization. Adv Colloid Interf Sci 79:149–172
29. Volpert E, Selb J, Candau F (1998) Associating behaviour of polyacrylamides hydrophobically modified with dihexylacrylamide. Polymer 39:1025–1033
30. Hill A, Candau F, Selb J (1993) Properties of hydrophobically associating polyacrylamides: influence of the method of synthesis. Macromolecules 26:4521–4532
31. Regalado EJ, Selb J, Candau F (1999) Viscoelastic behavior of semidilute solutions of multisticker polymer chains. Macromolecules 32:8580–8588
32. Kujawa P, Audibert-Hayet A, Selb J, Candau F (2006) Effect of ionic strength on the rheological properties of multisticker associative polyelectrolytes. Macromolecules 39:384–392
33. Tuncaboylu DC, Sari M, Oppermann W, Okay O (2011) Tough and self-healing hydrogels formed via hydrophobic interactions. Macromolecules 44:4997–5005
34. Tuncaboylu DC, Sahin M, Argun A, Oppermann W, Okay O (2012) Dynamics and large strain behavior of self-healing hydrogels with and without surfactants. Macromolecules 45: 1991–2000
35. Tuncaboylu DC, Argun A, Sahin M, Sari M, Okay O (2012) Structure optimization of self-healing hydrogels formed via hydrophobic interactions. Polymer 53:5513–5522
36. Can V, Kochovski Z, Reiter V, Severin N, Siebenbürger M, Kent B, Just J, Rabe JP, Ballauff M, Okay O (2016) Nanostructural evolution and self-healing mechanism of micellar hydrogels. Macromolecules 49:2281–2287

37. Bilici C, Can V, Nöchel U, Behl M, Lendlein A, Okay O (2016) Melt-processable shape-memory hydrogels with self-healing ability of high mechanical strength. Macromolecules 49:7442–7449
38. Argun A, Can V, Altun U, Okay O (2014) Non-ionic double and triple network hydrogels of high mechanical strength. Macromolecules 47:6430–6440
39. Su E, Okay O (2019) A self-healing and highly stretchable polyelectrolyte hydrogel via cooperative hydrogen-bonding as a superabsorbent polymer. Macromolecules 52:3257–3267
40. Flory PJ (1953) Principles of polymer chemistry. Cornell University Press, New York
41. Treloar LRG (1975) The physics of rubber elasticity3rd edn. Oxford University Press, Oxford
42. Durmaz S, Okay O (2000) Acrylamide/2-acrylamido-2-methylpropane sulfonic acid sodium salt-based hydrogels: synthesis and characterization. Polymer 41:3693–3704